



Original article

## A macroscale optimal substructure selection for Europe's offshore wind farms

Asier Vázquez<sup>a,\*</sup>, Urko Izquierdo<sup>a</sup>, Peter Enevoldsen<sup>b</sup>, Finn-Hendrik Andersen<sup>c</sup>,  
Jesús María Blanco<sup>a</sup>

<sup>a</sup> University of the Basque Country (UPV/EHU), Faculty of Engineering in Bilbao Department of Energy Engineering, Plaza Ingeniero Torres Quevedo 1, Bilbao 48013, Spain

<sup>b</sup> Centre for Energy Technologies, Department of Business Technology and Development, Aarhus University, Denmark

<sup>c</sup> Vestas Wind Systems A/S, Denmark



### ARTICLE INFO

#### Keywords:

Offshore wind energy  
Multi-Criterion Decision Making  
Geographic Information System  
Site selection  
Offshore wind potential

### ABSTRACT

Considering the political decisions taken in Europe in the last year, there is a renewed interest in the offshore wind sector. A considerable growth of large-scale offshore wind farms (OWF) is noticeable in Europe mainly due to technological advances in wind turbines and foundation structures, which have reduced their costs and improved their performance, and contributed to the implementation of offshore plants. This study uses a Multi-Criterion Decision Making (MCDM) approach in a Geographic Information System (GIS) to analyze which type of foundation is more adequate according to water depth, soil, and wave conditions, as these parameters affect not only the viability of the foundation type but also on the Levelized Cost of Energy (LCoE) of wind energy of the European seas. The results highlight the importance of floating offshore wind, as 61.55% of the total area could be exploited by these means. Moreover, the current exploited power could be increased by a factor of 615. The validation of the obtained results with up-to-date empirical data confirms the accuracy of this study and shed light on the importance of offshore wind, what could encourage policymakers on their decision-making process.

### Introduction

The offshore wind industry has expanded over the past three decades since the first installation in Denmark in 1991 [1]. The expansion has resulted in offshore installations in more than 50 countries with a cumulative capacity of 55.7 GW. The majority of the global offshore installations are located in Europe (27.8 GW) [2]. However, China was the leading offshore market in 2021, and the projections in North America and South-East Asia involve staggering numbers from 5 to 30 GW in a few years. Fig. 1 illustrates the global offshore installations at the end of 2021.

Moreover, the size of offshore wind turbines has increased as highlighted by [3] from 1.5 MW installed capacity in 1998 to double-digit turbines proposed in 2019, and turbines with higher capacity than 8 MW. A similar development has been observed for the rotor diameter and hub height, with 164 m and 142.5 m, respectively, as the greatest commercial installed numbers [3]. The increase in the size of offshore wind turbines is a technological development driven by the aim of decreasing the LCoE, which can be obtained at 0.14 \$/kWh in 2019;

however, with a record low bid of 0.06 \$/kWh [4]. In [5] the overall CAPEX (Capital Expenditure) breakdown of an installed offshore wind turbine is calculated, which is presented in Fig. 2.

In [5] it is further concluded that foundation costs have a sensitivity range from 20 % to 30 % of the CAPEX. The design of a foundation is primarily determined by the selected wind turbine, and then, depth and soil conditions are taken into consideration [6]. In continuation, [7] found that offshore wind projects come with a greater risk of cost overrun and delays than onshore, and further that the cost overrun can be divided based on foundation types. The study found that projects where gravity-based foundations are introduced have a mean cost overrun of 5.4 %, projects with monopiles have a mean cost overrun of 7.4 %, and other types including jackets, tripods, etc. come with a mean cost overrun of 24.7 % [7]. Given the importance of the foundation type, which is driven by environmental conditions such as water depth, it is interesting to focus on the water depth of the installed offshore wind projects. Fig. 3a presents such overview of 112 installed wind farms accounting for a total of 17.77 GW, which corresponds to approximately 77 % of the world's installed offshore wind capacity by 2020.

Furthermore, when estimating the weighted average of the 112

\* Corresponding author.

E-mail address: [avazquez059@ikasle.ehu.eus](mailto:avazquez059@ikasle.ehu.eus) (A. Vázquez).

| Nomenclature   |                                                          |                      |                                               |
|----------------|----------------------------------------------------------|----------------------|-----------------------------------------------|
| <i>Letters</i> |                                                          | <i>Greek symbols</i> |                                               |
| CAPEX          | Capital Expenditure                                      | GWEC                 | Global Wind Energy Council                    |
| $C_F$          | cost of foundation                                       | $H_S$                | significant wave height [L]                   |
| CRS            | Coordinate Reference System                              | IRENA                | International Renewable Energy Agency         |
| $d$            | grain size [L]                                           | J                    | Jacket                                        |
| $D$            | water depth [L]                                          | LCoE                 | Levelized Cost of Energy                      |
| ECMWF          | European Centre for Medium-Range Weather Forecasts       | M                    | Monopile                                      |
| EMODnet        | European Marine Observation and Data Network             | MCDM                 | Multi-Criterion Decision Making               |
| ETIP           | European Technology & Innovation Platform on Wind Energy | OWF                  | Offshore Wind Farm                            |
| FOW            | Floating Offshore Wind                                   | $P$                  | wave energy flux [ $M \cdot L \cdot T^{-3}$ ] |
| FOWT           | Floating Offshore Wind Turbine                           | S                    | spar-type support                             |
| $g$            | acceleration of gravity [ $L \cdot T^{-2}$ ]             | SS                   | Semi-submersible                              |
| GB             | Gravity-based                                            | T                    | Tripod                                        |
| GIS            | Geographic Information System                            | $T$                  | wave period [T]                               |
|                |                                                          | TLB                  | Tension Leg Buoy                              |
|                |                                                          | $\rho$               | density [ $M \cdot L^{-3}$ ]                  |

installed wind farms, it is found that the mean water depth per installed MW is 23.2 m. This corresponds with the study from [6] stating that the most used foundation type are monopiles, which usually fit with such water depth. Nevertheless, an overview of future offshore wind projects has also been performed, based on the information from [8], indicating the water depths for 201 wind farms with a status of ‘approved’, ‘planned’, or ‘under construction’ and a project installed nameplate capacity of 101 GW. Fig. 3b presents the division of projected MW for different groups of water depths.

The weighted mean water depth per projected MW of offshore wind power is estimated to be 29.3 m, which indicates a shift towards wind turbines being installed at greater depths. Nonetheless, this depth would not be considered sufficient for applying floating foundations.

In general, floating foundations are considered the economic best fit for water depths exceeding 50 m [9] or in some cases 70 m [10]. Nevertheless, when investigating the European offshore potential, [10] found that in 2030 more than 2,500 TWh/year could come from offshore wind turbines with floating foundations. To achieve these numbers, [11] expects Europe to install 116 GW in the period between 2022 and 2026. Similar results were stated for the US, as [12] included an offshore additional harnessable area of 551,717 km<sup>2</sup> when considering water depths in the range of 60–700 m. Such area would be converted into a

theoretical potential of 3,972 GW, according to a spacing density of 7.2 MW/km<sup>2</sup>, which is the average of 969 operating offshore wind turbines in Europe [13].

It is, however, doubtful whether the business case will be likely to be established at very great water depths, yet, in 2020, Siemens Gamesa Renewable Energy, Innogy, Shell, and Stiesdal Offshore Technologies planned to install a 3.6 MW wind turbine with the Tetra Spar floating foundation at a water depth of approximately 200 m in Norway [14], which is currently hooked to Norwegian mainland. In California, the introduction of floating foundations is expected to increase the offshore potential from approximately 15 GW to 573 GW. Similar conclusions can be drawn globally, as several studies have examined the potential and requirement of applying floating foundations in Taiwan, Japan, and South Korea, indicating impressive potential [15,16]. Despite being a novel technology, several commercial projects have been planned, and a number of those projects have been presented in Table 1.

There is a potential for floating foundations, and studies have proven the improved LCoE of utilizing floating foundations at great water depths [9,17]. However, few, if any studies have adequately examined which offshore substructure to use. In lack of response, if any, this study aims to develop such an overview for Europe indicating the wind power potential that come with each substructure technology.

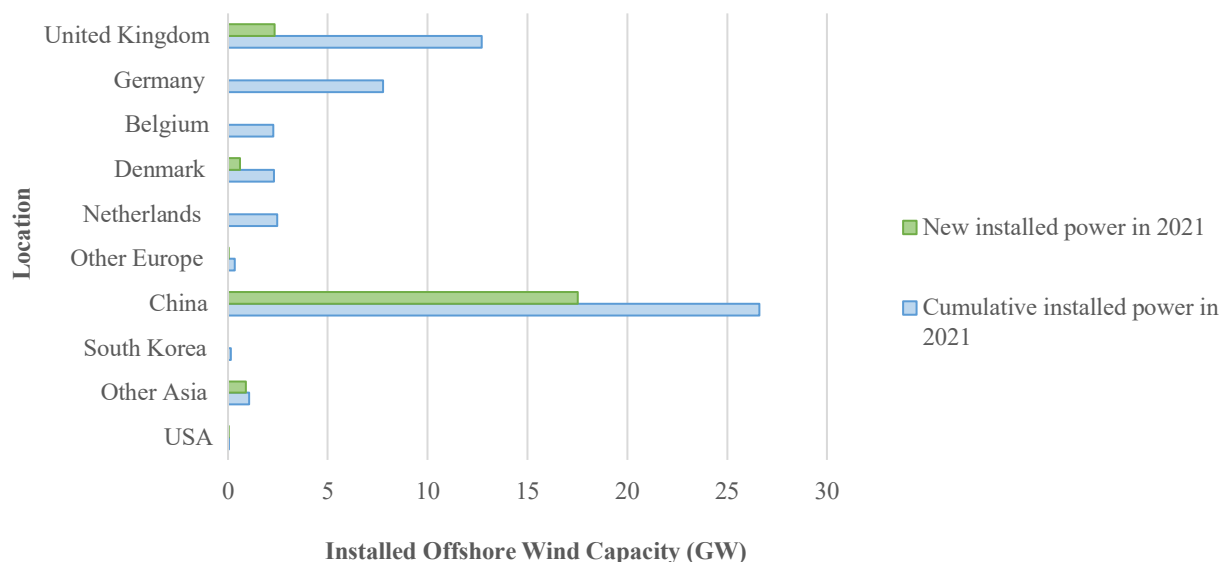


Fig. 1. Global installed offshore capacity (GW), based on data from [2].

The objective of this study is to provide a map of European seas in which the most adequate offshore wind foundation to use is shown, aiming to facilitate a decision-making process. The work is based on a multi-variate analysis, considering water depth, soil substrate type, wind speed and wave energy flux as influencing parameters. To this end, initially, a literature review has been performed, enabling to generate a decision matrix which has further been used in the obtaining of results.

### Research methods and materials

To determine the most adequate type of foundation over all European seas, several variables and parameters have been considered, as they are water depth, type of soil substrate, and wind and wave conditions. The former fall under the so-called geotechnical conditions, while the latter are part of met-ocean conditions. All the parameters were considered according to the limitations presented by the existing type of foundations. The geotechnical conditions take all parameters that are related to the seabed into consideration, such as the depth with respect to sea level or, more directly, the type of substrate and its characteristics: porosity, grain size distributions, etc. [18]. As stated by [19], the type of substrate affects the load-bearing capacity, hence it is crucial to make the right substructure selection to maximize the life span of the wind farm. On the other hand, the term “met-ocean” refers to the combined effect of meteorology and oceanography. Therefore, met-ocean conditions are those in which both meteorological and oceanographic conditions, including local surface winds, wind-generated local waves, swell waves, etc. are considered [20].

### Selection of the design input parameters

In this study, the geological information is provided by EMODnet (European Marine Observation and Data Network) [21]. It offers bathymetric data for areas comprised between latitudes of 15° N and 90° N, and longitudes of 36° W and 43° E, covering the whole European maritime area with a grid size of 0.125° x 0.125°. Moreover, seabed substrate information from the period comprehended between 2009 and 2021 is provided for an area comprised between latitudes of 23° N and 83° N, and longitudes of 30° W and 68° E, approximately. The data has been mapped with a scale of 1:1,000,000 and in the basis of the Folk 5 triangle [22]. The Folk scheme classifies the sediment based on the sediment fractions of mud (grain size  $d < 63 \mu\text{m}$ ), sand ( $63 \mu\text{m} \leq d < 2 \text{mm}$ ) and gravel ( $d \geq 2 \text{mm}$ ). The simplification of this scheme, from the

original 15 sediment classes to six and four (for Folk 7 and Folk 5, respectively), allowed the harmonization of the European seabed substrate data into a unified substrate map. Thus, four classes are represented (mud to muddy sand; sand; coarse substrate; and mixed sediment) on the simplest modified Folk triangle, to which a fifth one (rock & boulders) was added by the project team.

On the other hand, the wind conditions dataset used for this study, published in [23], provides information with an offshore coverage of 200 km from the shoreline for the period comprehended between 2008 and 2017. The modeling system used presents a horizontal grid spacing of 250 m and data is compiled at heights of 10, 50, 100, and 200 m above the sea level.

Concluding with met-ocean conditions, significant wave height, which represents the average height of the highest third of surface ocean waves generated by local winds and associated with swell, and period ( $H_s$  and  $T$  respectively) were acquired from ERA5 [24], allowing to calculate the total wave energy flux. This information is based on a reanalysis dataset by the European Centre for Medium-Range Weather Forecast (ECMWF) for the period between 2010 and 2020, with an hourly time frequency and a spatial resolution of 0.5°. The maximum individual wave height is an estimation of the expected highest individual wave within a 20-minute time window. The interactions between waves are non-linear and occasionally concentrate wave energy, giving a wave height considerably larger than the significant wave height. In addition, the period which has been considered is the one associated to those maximum individual wave heights. A summary of the utilized datasets, as well as the representations of these, are shown in Table 2 and Fig. 4, respectively.

### Influence of geotechnical conditions on substructure selection

The fixed foundations have been differentiated into monopiles, jackets, tripods, gravity-based structures, buckets, and tripiles. Nonetheless, the latter two were not considered in this study as they are not frequently used in European offshore wind farms [8]. A representation of the various fixed and floating concepts is shown in Fig. 5. The monopiles are the most used type of foundation in Europe, with an accumulative of 81.2 % [25]. They have been relevant for water depths down to 30 to 50 m; however, in the case of XXL monopiles they could be installed in depths down to 70 m [26]. Jackets and tripods are mainly used at depths between 25 and 60 m and represent the 9.9 % and 2.2 % of all European OWFs respectively [25]. Both are economically more

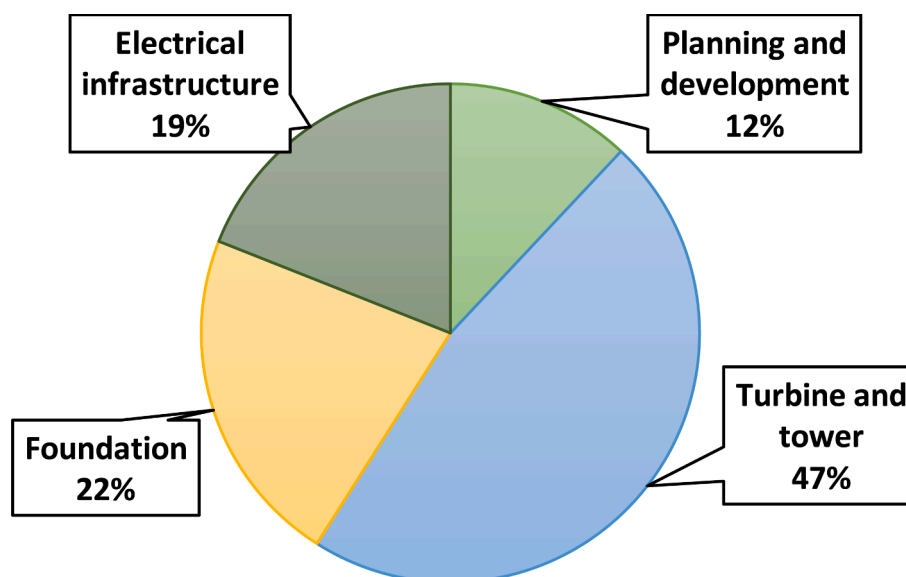


Fig. 2. CAPEX breakdown of an installed offshore wind turbine [5].

feasible at increasing depths, thus, they are not usually recommended for shallower waters [26]. Finally, the gravity-based structures represent the 5 % of all OWFs in Europe [25]. Although they can be built down to 60 m, they are most often used in shallow waters down to 20 m. The fact that this technology is proven and adapted from oil & gas industries makes it a secure type of installation, which was mainly used in shallow European wind farms during the last decade [26,27].

In the case of floating foundations, the criteria established by [28], [29] and [30] have been considered for each of these foundations. ETIP (European Technology & Innovation Platform on Wind Energy) ascertains semi-submersibles can be used for water depths below 40 m, while barges, which are also stabilized by their buoyancy, could be installed at even shallower water (30 m). In the case of Tension-Leg-Buoys (TLB), they fix their minimum depth at 50 m; whereas for spar-type supports this corresponds to 100 m. On the other hand, IRENA (International Renewable Energy Agency) has determined a similar criterion to the aforementioned one for semi-submersibles. According to this entity, TLBs can be used in water depths from 50 to 60 m, while spar-type supports need deeper waters (100 m). Lastly, ETIP establishes the minimum depth for semi-submersibles and TLBs at 50 m, and at 80 m for spar-type supports. All in all, the water depth ranges at which the different foundations described could operate are graphically plotted in Fig. 6.

Nonetheless, floating wind technology cannot extend beyond some practical depth limit. There is no industry-wide consensus on the maximum depth that floating wind plants might reach. Up-to-date, researchers affirm that this bond must be somewhere between 700 and 1,300 m. This limit is somehow based on economic criteria, but there is some concern that subsea cables could not be suitable below a 1,300 m depth. However, many researchers and developers believe that 1,000 m is a more appropriate depth at which to establish this lower limit [12,32,33].

Fixed foundations are mainly affected by geotechnical conditions, among which the type of soil substrate has a notorious influence. On the other hand, although floating foundations do not depend so much on the aforementioned conditions, there is still some effect on whether the most adequate substructure is a semi-submersible, TLB or spar-type one. Due to these differences between fixed and floating foundations, the influence of soil substrate will be analyzed independently for both types. The main advantage of monopiles is that they can be used in many bottom conditions, such as stone mixed bottoms, sand, or clay where there is an underlying solid bed. The principal limitation for this type of foundation

**Table 1**  
Commercial offshore wind projects applying floating foundations.

| Project                            | Country        | MW | Year |
|------------------------------------|----------------|----|------|
| Hywind                             | Scotland       | 30 | 2017 |
| Windfloat Atlantic                 | Portugal       | 25 | 2019 |
| Flocan 5                           | Spain          | 25 | 2020 |
| Nautilus                           | Spain          | 5  | 2020 |
| SeaTwirl S2                        | Sweden         | 1  | 2020 |
| Kincardine                         | United Kingdom | 49 | 2020 |
| Forthwind Project                  | United Kingdom | 12 | 2020 |
| EFGL                               | France         | 24 | 2021 |
| Groix-Belle-Ile                    | France         | 24 | 2021 |
| PGL Wind Farm                      | France         | 24 | 2021 |
| EolMed                             | France         | 25 | 2021 |
| Katanes Floating Energy Park-Array | United Kingdom | 32 | 2022 |
| Hywind                             | Tampen         | 88 | 2022 |

**Table 2**  
Summary of the datasets employed.

| Parameter of analysis             | Dataset               | Period of analysis | Spatial resolution |
|-----------------------------------|-----------------------|--------------------|--------------------|
| Water depth                       | EMODnet               | 2021               | 0.125°             |
| Soil substrate                    | EMODnet               | 2009–2021          | –                  |
| Mean wind speed and power density | The Global Wind Atlas | 2008–2017          | 250 m              |
| Wave height and period            | ERA5 (ECMWF)          | 2010–2020          | 0.5°               |

is the rocking stiffness, so it is not recommendable when there is a high density of boulders or at rocky bottoms, as the cost would increase due to the necessity of drilling. Moreover, in the Baltic Sea, for example, the heavy weight stress from ice is a disadvantage for this technology, and therefore, costs are more expensive in these areas compared to other ice-free areas [26,27,34]. Gravity-based foundations can be adapted to a variety of bottom substrates by adjusting the base diameter because this kind of foundation does not require a deeper recess in the bottom substrate. This implies that gravity foundations are well suited for rocky bottoms and bottoms with boulders, as well as stable (well-packed) sediments. Bottoms of consistently loose sediment are on the contrary not appropriate for the gravity foundations. Moreover, clay and unstable sand are not really suitable for this type of foundation [27,34]. Finally, jackets and tripods can be used in nearly all types of soils, being especially effective in stiff clays and medium-to-dense sands, although it is also possible to install them in softer soils. However, tripods present

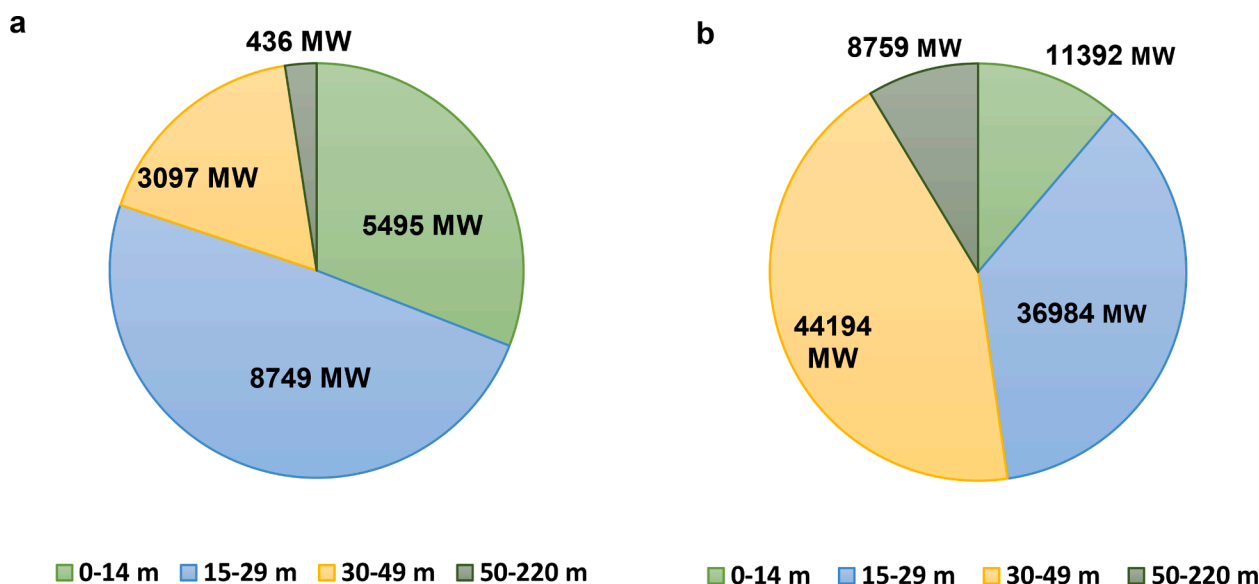


Fig. 3. a) Water depths for installed offshore wind farms, b) Water depths for future offshore wind farms. Based on data from [8].

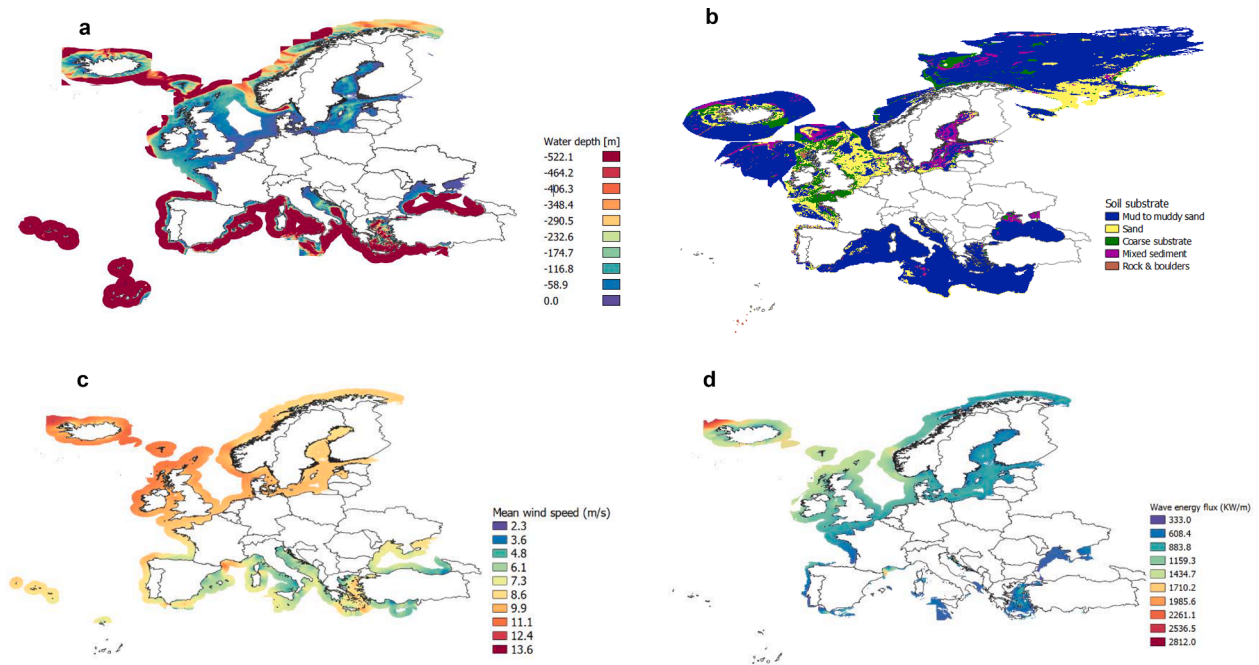


Fig. 4. Representation of the datasets for the area of study. a) Water depth, b) Soil substrate, c) Mean wind speed, d) Wave energy flux.

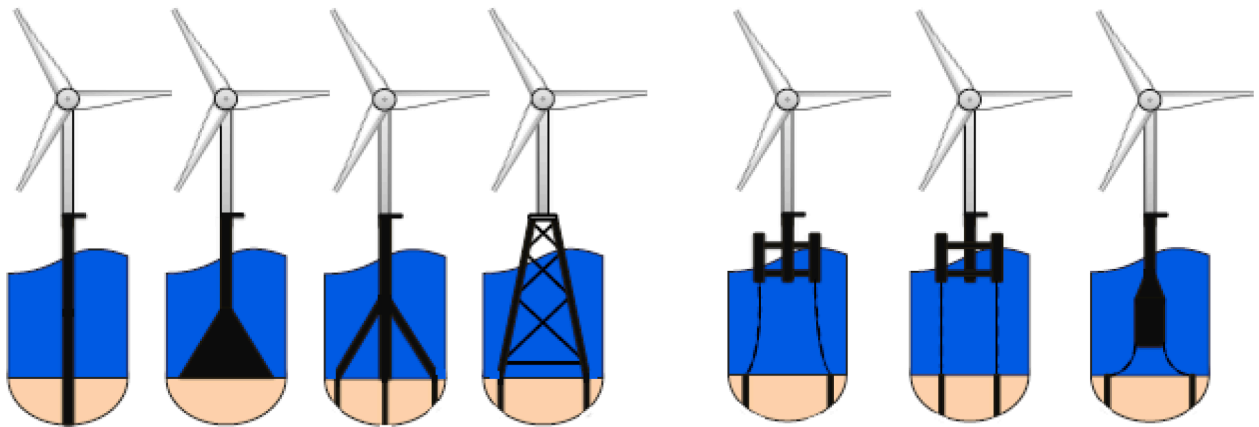


Fig. 5. Different fixed and floating foundations for offshore wind farms. From left to right: monopile, gravity-based, tripod, jacket, semi-submersible, TLB, and spar-type support [31].

inconveniences due to the piling in areas with a lot of boulders or completely rocky seabed [27,34]. The possibility to be installed in different types of soils is due to the fact that they can be established with piles or with suction caissons [35].

In the case of floating foundations, geotechnical conditions are an important factor in determining the anchoring system that can be used. Cohesive soils that are not too stiff, but also not too loose are the most favorable ones to allow certain flexibility in the selection of the anchoring system. In that sense, the decision is an economic one, but in this case, the importance lies in the anchor type that is used. Anchor costs are generally higher for TLBs, as there is a need to withstand high vertical loads and maintain platform stability [36]. The main anchor types used are drag-embedded anchors, gravity anchors, driven piles, and suction piles. The latter have only been proved in soft soils, whereas the other three have concepts in both, hard and soft soils. Gravity and driven anchors, with suction anchors in soft soils, are the only ones that can be used for TLBs, and these three are the ones with a larger cost per unit. Due to this reason, several studies have concluded that, while semi-submersible and spar-type supports are insensitive to soil conditions,

TLBs are unsuitable for challenging soil conditions [37–41].

*Influence of met-ocean conditions on substructure selection*

Wind speed is not a parameter directly related to the use of a particular technology. This parameter will serve as a basis to determine if a certain area has an adequate energetic potential so that wind farms could be economically feasible, however, wind and wave misalignments will impact the substructure and tower design, while overall wind conditions will have an impact on the tower and therefore indirectly impact the substructure [6]. Nevertheless, to develop a quantitative analysis, it is fair enough to establish a lower limit for mean wind speeds, from where it would not be recommended to execute an OWF project; thus, average wind speed will be used as a discriminatory parameter. Following the business aspect justifications presented in [42], a minimum wind speed of 7 m/s will determine which areas will be excluded from this analysis [12]. Moreover, the decision of establishing the minimum speed at 7 m/s can be validated by analyzing the situation of European Offshore Wind Farms. According to the data obtained from



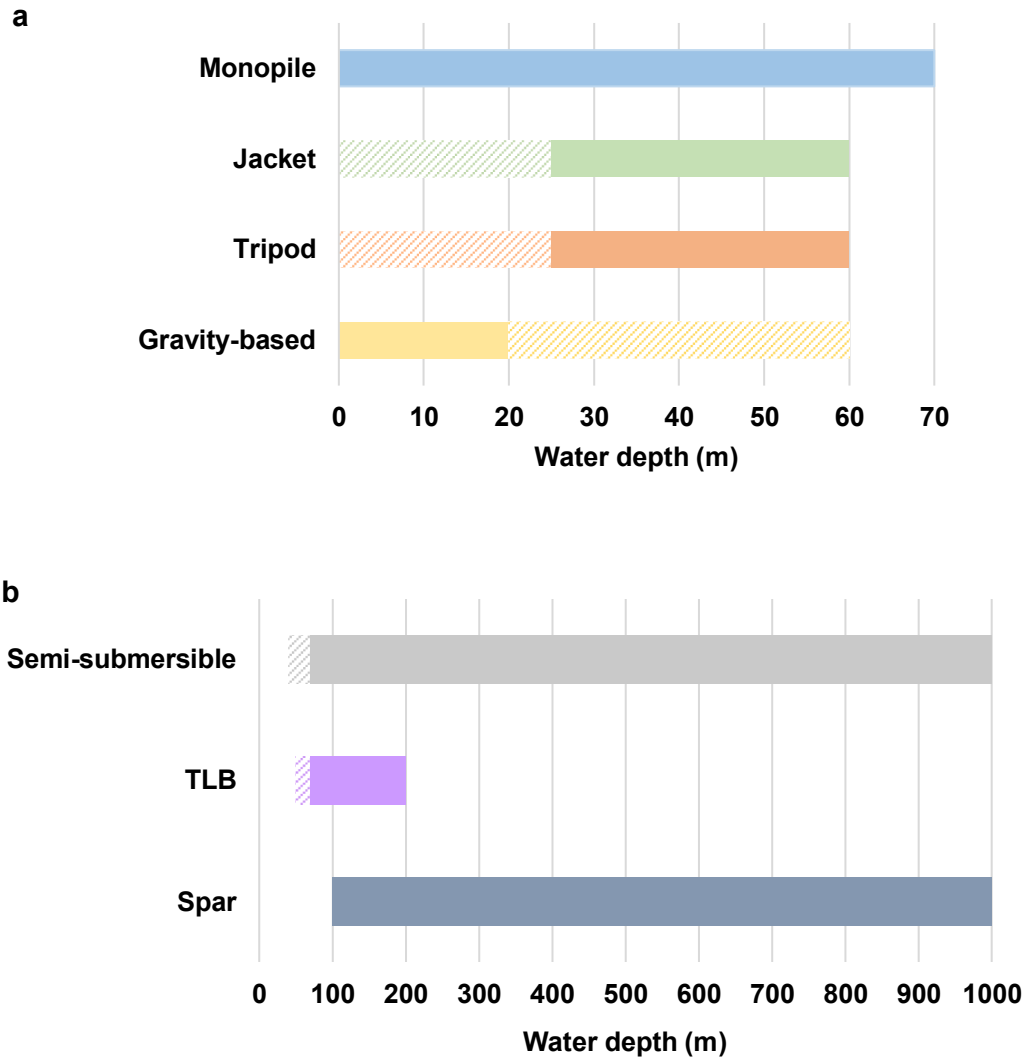


Fig. 6. Water depth ranges at which offshore wind foundations might operate. a) Fixed foundations, b) Floating foundations.

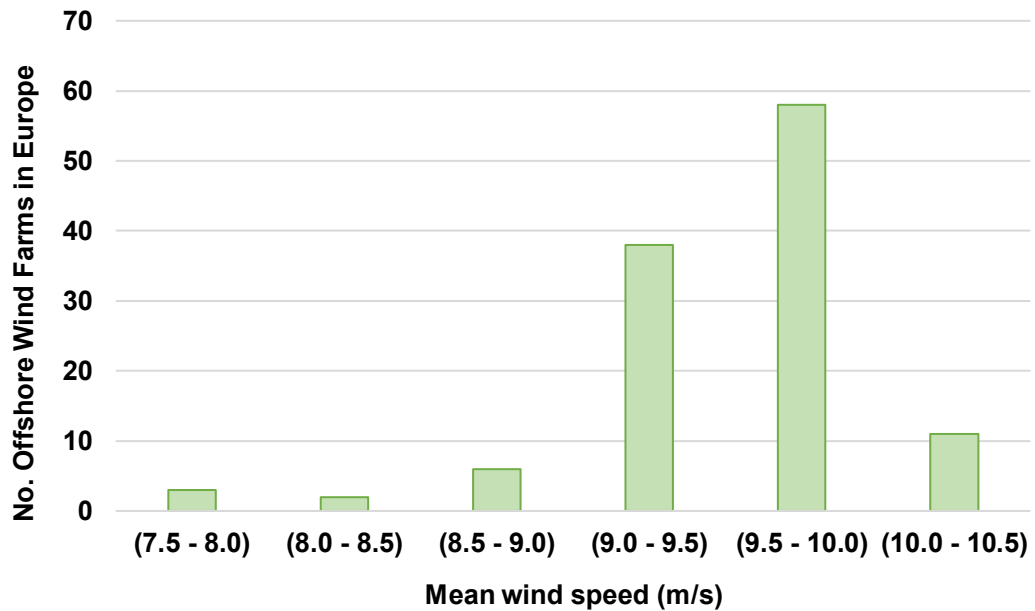


Fig. 7. Number of European offshore wind farms as a function of the average wind speed at their location.

[43], the minimum average speed for all European Offshore Wind Farms is registered in Portugal's Wind Float Atlantic with a value of 7.7 m/s, while the largest one (10.1 m/s) is obtained at Riffgat in Germany, Horns II and III in Denmark, and Hywind Scotland Pilot Park in the United Kingdom. As plotted in Fig. 7, the mean speed in most European OWFs is somewhere in between 9 and 10 m/s. Therefore, areas with mean wind speeds below 7 m/s have not been considered in this study, as they would not be of particular interest from an economical point of view due to their low wind harnessing capacity.

It is worth to mention that the data from [43] has been obtained for a height of 100 m. An analysis of current European OWFs' hub height has been executed to calculate the average height at which the rotors are located. The mean hub height of the 108 studied OWFs is located at 85.3 m. Moreover, considering that future turbines will be located higher, as trends show [3], it seems to be interesting to carry out the analysis based on data at 100 m above the sea level.

Finally, specific wave parameters have been considered, which may exclude some types of substructures in certain areas. Met-ocean conditions have a greater influence on floating structures [44], being practically negligible in the case of fixed structures, where the geotechnical conditions described so far have a greater effect. In this context and considering the information available in the ERA5 database [24], which offers information on maximum wave heights and the periods associated with these waves, a literature review has been carried out to determine which conditions could be considered extreme and detrimental to the stability and resistance of the floating structures. In this way, the excluding parameter would be the wave energy flux or wave power, which is a function of the two variables, wave height and wave period, mentioned above.

The wave power, in deep water areas where the water depth is larger than half the wavelength, can be obtained through Eq. (1) [45]:

$$P = \frac{\rho}{64} \frac{g^2}{\pi} H_s^2 T \approx 0.5 \frac{H_s^2 T}{m} \text{ kW} \tag{1}$$

It is noteworthy that, in this analysis, all the areas will be considered as deep water, as this parameter is considered excluding in areas where floating structures will be located, as they are areas with water depths exceeding 70 m.

In [46] an experimental and computational analysis for a spar-type floating offshore wind turbine was developed. According to this study, extreme conditions were tested for regular waves with  $H_s = 10$  m and  $T = 15$  s, while these conditions for irregular waves were fixed at values of  $H_s = 14.4$  m and  $T = 13.3$  s. A similar analysis was executed in [47] but for various FOWTs (Floating Offshore Wind Turbines), as they are TLBs, semi-submersibles, and spar-type supports. In this case a more conservative criterion has been established, fixing maximum heights and periods of  $H_s = 6.4$  m and  $T = 14$  s, respectively for regular waves, and  $H_s = 8.7$  m and  $T = 12.4$  s in the case of irregular waves.

Lastly, the study for TLBs, semi-submersibles, and spar-type supports by [48] has been considered. This analysis only considers irregular waves, fixing a limit in wave heights and periods of  $H_s = 10$  m and  $T = 14$  s, respectively.

All these criteria, together with the resultant wave power that can be

**Table 3**  
Review of extreme wave conditions [46–48].

| Authors        | Significant wave height, $H_s$ (m) | Wave period T (s) | Wave regime | Wave power (kW/m) |
|----------------|------------------------------------|-------------------|-------------|-------------------|
| Yang, et al.   | 10.0                               | 15.0              | Regular     | 750.00            |
| Yang, et al.   | 14.4                               | 13.3              | Irregular   | 1378.94           |
| Chuang, et al. | 6.4                                | 14.0              | Regular     | 286.72            |
| Chuang, et al. | 8.7                                | 12.4              | Irregular   | 469.28            |
| Collu and Borg | 10.0                               | 14.0              | Irregular   | 700.00            |

calculated by applying Eq. (1) are shown in Table 3.

Considering this review, quite a conservative criterion will be established, as it is always possible to build larger structures that could bear bigger wave loads. Nevertheless, an economic analysis should be performed in this case. All in all, extreme waves will be considered with wave heights and periods exceeding values of  $H_s = 15$  m and  $T = 14$  s, with an overall energy flux or power of  $P = 1575$  kW/m, so that all areas where energy fluxes exceed these values will be considered inadequate.

Considering all the criteria that have been exposed until now, it is adequate to develop a decision matrix in which all the parameters are contemplated (see Table 4). This will serve as a summary of all the analyses that have been performed.

Floating structures are rejected in the areas where wave power exceeds 1575 kW/m. Moreover, only areas with an average wind speed larger than 7 m/s will be considered in this analysis.

*Using GIS to map the optimal substructure selection*

In the previous part, the criteria of selecting the optimal substructure for offshore wind farms have been established. In order to determine where in the study area which substructure is most applicable, a spatial form of MCDM in a GIS is used. A GIS is used to obtain geo-referenced results for a multivariate study. Moreover, a MCDM analysis can be widely used in various fields, as extracted from [49,50]. In this case, the different criteria are determined by the input datasets which are datasets in layer form whose values are spatially distributed. In a GIS, these different data layers can be combined using geo-processing algorithms to spatially assess the applicability of each substructure based on the criteria established. As this research is promoting free and open source data and tools, QGIS was used for the calculations [51]. The different geo-processing steps used in QGIS to calculate a resulting layer showing the spatial distribution of substructure applicability are outlined in this subsection.

First, the data has to be pre-processed to harmonize the various layer extensions and the data format of the layers, showing the criteria for decision-making. Table 5 is showing the layers used, including their extension and Coordinate Reference System (CRS).

The GDAL Warp algorithm in QGIS was used to crop the extent of the layers to the same matching the study area and re-project to LAEA Europe EPSG:3035 for the GDAL algorithms to run, since they require metric units. The outcome of this processing steps are 5 different raster layers and one vector layer with the same CRS and extend. A schematic

**Table 4**  
Decision matrix for the determination of offshore wind foundations as a function of water depth and soil substrate type.

|                 |            | Soil substrate    |              |                  |                |                 |
|-----------------|------------|-------------------|--------------|------------------|----------------|-----------------|
|                 |            | Mud to muddy sand | Sand         | Coarse substrate | Mixed sediment | Rock & boulders |
| Water depth (m) | 0 – 20     | M                 | GB – M       | GB – M           | M              | GB              |
|                 | 20 – 25    | M                 | M            | M                | M              | –               |
|                 | 25 – 60    | M – J – T         | M – J – T    | M – J – T        | M – J – T      | J               |
|                 | 60 – 70    | M                 | M            | M                | M              | –               |
|                 | 70 – 100   | SS – TLB          | SS – TLB     | SS – TLB         | SS – TLB       | SS – TLB        |
|                 | 100 – 200  | SS – TLB – S      | SS – TLB – S | SS – TLB – S     | SS – TLB – S   | SS – TLB – S    |
|                 | 200 – 1000 | SS – S            | SS – S       | SS – S           | SS – S         | SS – S          |

\* M: monopile, GB: gravity-based, J: jacket, T: tripod, SS: Semi-Submersible, TLB: Tension-Leg-Buoy and S: spar-type support.

**Table 5**  
Details of layers used.

| Layer                             | Source                | Extent                             | CRS [EPSG] | Data Format |
|-----------------------------------|-----------------------|------------------------------------|------------|-------------|
| Country borders                   | GADM                  |                                    | 4326       | Vector      |
| Water depth                       | EMODnet               | -34.169, 25.842: 43.000, 73.199    | 4326       | Raster      |
| Soil substrate                    | EMODnet               | -30.870, 23.680: 68.030, 81.852    | 4326       | Raster      |
| Mean wind speed and power density | The Global Wind Atlas | -180.331, -58.322: 180.327, 81.511 | 4326       | Raster      |
| Wave height and period            | ERA5 (ECMWF)          | -180.331, -58.323: 180.327, 81.511 | 4326       | Raster      |

data flow can be seen in Fig. 8 and Fig. 9.

In the following, different algorithms are used to process the data layers in QGIS. Hereby, especially the Raster Calculator was used. The Raster Calculator is a spatial processing tool in QGIS that calculates mathematical equations and trigonometric functions using the pixel or cell values of raster layers. It can also be used for working with conditional expressions which return binary values. Hence, those expressions can be used to create masks based on a certain condition, which in turn can be combined to a single output file based on multiple criteria. Using the different raster bands of the input layers and the Raster Calculator syntax the result layer, which fulfills all conditions of the decision matrix, was calculated.

In more detail, the following algorithms were used to pre-process the different layers to be used in the decision matrix. The Country Borders layer was *buffered* with a distance of 150 km outlining the study area as defined earlier on. The Soil Substrate layer was *re-classified* using a raster calculator expression from the initial 15 classes into 5. The mean wind speed layer was *masked* with a value higher or equal to 7 m/s and the Wave Height and Wave Period layers were used to *calculate* in the raster calculator the Wave Power layer using Eq. (1). The Buffered Borders layer was then used as a mask to *crop* the 5 Soil Substrate Classes layer. The resulting layer was used in the raster calculator together with the Mean Wind Speed  $\geq 7$  m/s layer as a *mask*. The resulting layer was used in another raster calculator expression with the Wave Power layer as a *mask* to create the final Soil Substrate layer. This layer was used together with the Water Depth layer in a raster calculator expression

classifying all cell values according to the decision matrix in this step also all values above 1000 m in the Water Depth layer were *masked*.

## Results and discussion

### Analysis of the theoretically exploitable area

The most adequate type of offshore wind foundation has been established based on the criteria previously determined (water depth, soil substrate type, wind speed, and wave energy flux) for the study area, which comprises the first 150 km from the shore, always in water depths until 1,000 m. The distribution of the different types of foundations is plotted in Fig. 10. Attending to the parameters considered, the overall European offshore area in which wind turbines could be theoretically located is 2,134,812 km<sup>2</sup>. An analysis has been made to quantify the influence of each parameter in the determination of the exploitable area. If only established water depth conditions were to be considered, that is, areas shallower than 1,000 m and at a maximum distance of 150 km offshore, an area of 3,217,106 km<sup>2</sup> could be harnessed by offshore wind turbines. If the minimum wind speed condition is introduced, the possible area decreases to 2,627,284 km<sup>2</sup>. And, finally, establishing the maximum wave energy flux value, the initially introduced area is obtained. The decomposition of this final area in the different groups of substructures that have been analyzed in depth, and the results, are shown in Fig. 11.

Visually examining Fig. 10, the largest areas are in the Baltic and North seas, as the depth in these areas is quite shallow even at big distances from the shoreline. Following the existing trend to move towards deeper waters, the results demonstrate the need to rely on floating structures, as these could theoretically be located in the 61.5 % of the area selected by this study. This move in favor of floating structures would make it possible to harness offshore wind resources in hitherto unexplored locations with great potential, such as the North-West coast of Spain or areas of the Mediterranean Sea between North-East Spain and South-West France, where wind potential is comparable to the most energetic areas in the North Sea (Fig. 12). Moreover, areas around the Orkney Islands (Scotland) and the South-West coast of Norway could also be explored by means of floating structures. Nonetheless, considering the costs associated with the exploitation of this resource, the greatest feasibility is currently achieved in the North Sea, off the Dutch and British east coast, and in areas of the Baltic Sea, off the Danish coast,

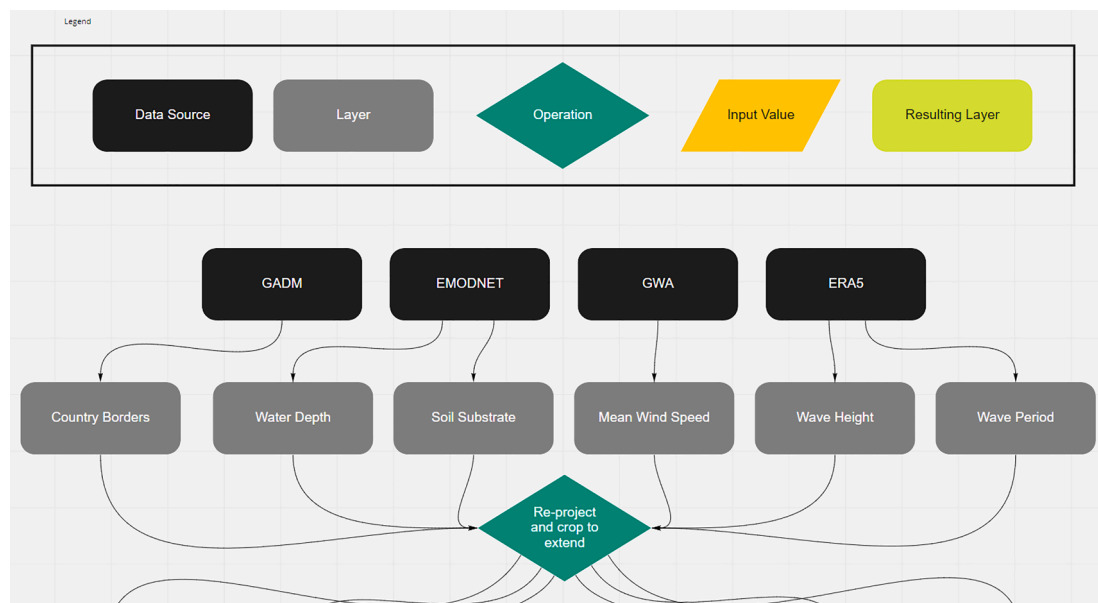


Fig. 8. Schematic data flow (part I).



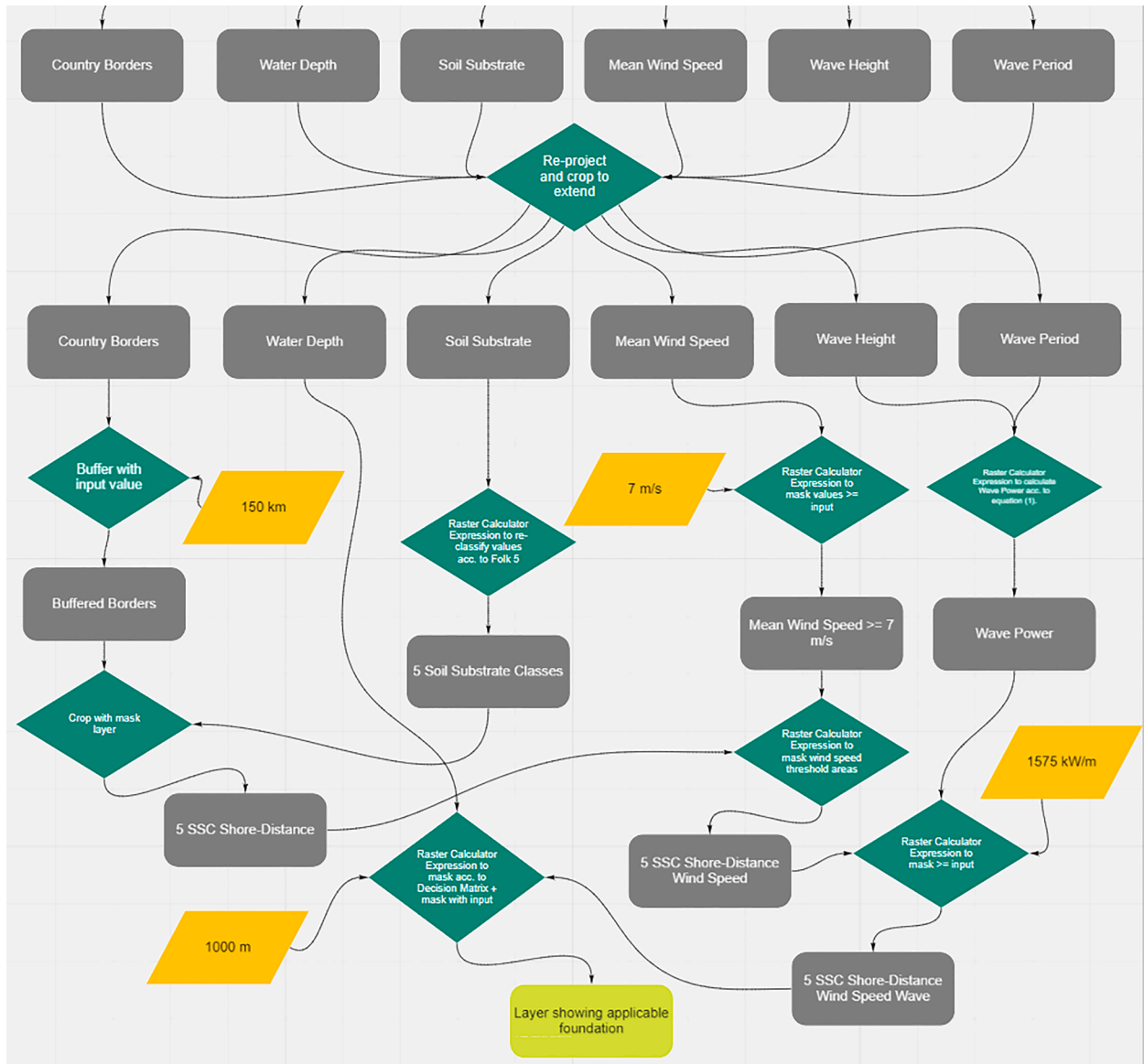


Fig. 9. Schematic data flow (part II).

where the possibility exists to deploy bottom-fixed structures such as monopiles or jackets.

*Distribution of foundation types*

Based on the results obtained, the main substructures to be used would be monopiles in the case of areas where bottom-fixed structures are suitable and semi-submersible structures if, due to the depth, floating structures must be chosen. This is in line with current trends, as more than 80 % of turbines in offshore wind farms in Europe are based on a monopile [25]. Furthermore, the commitment to semi-submersibles in this article is supported by GWEC (Global Wind Energy Council) [52]. Based on their latest report, semi-submersibles appear to be the most popular floating substructure, being projected to be installed in 64 % of the FOW (Floating Offshore Wind) projects at development stage. This is due to their independence with respect to depth and substrate type, their stability, and the wide variety of mooring and anchoring systems they allow. Despite their complex construction, they offer a high potential for modularization, which would facilitate mass production.

Considering that the mean output power density of offshore wind farms in Europe is  $7.2 \text{ MW/km}^2$  [13], the total exploitable power that

theoretically might be obtained is 15.37 TW. This would increase the current installed offshore wind power capacity by a factor of 615. Fig. 13 shows a graphic representation of the total exploitable power for each group of foundations.

In this respect, the power density of the different areas considered could be an indication of suitability when starting an offshore wind project. Several studies [53–55] have carried out a site selection process for floating substructures in different regions of Europe, by analyzing the LCoE of the technology. They conclude that the regions in which wind energy harnessing is the most efficient are those obtained by this study. However, although this study does not consider the economic aspect, it determines the type of substructure to be used, which would offer a greater level of detail in terms of costs, since, according to [55], the turbine and substructure account for ~50 % of the overall cost.

If each foundation is analyzed separately, the obtained results are shown in Fig. 14. From these results it is evidenced that monopiles, in the case of fixed structures, and semi-submersibles, for floating structures, should lead production in the coming years. Fig. 15.

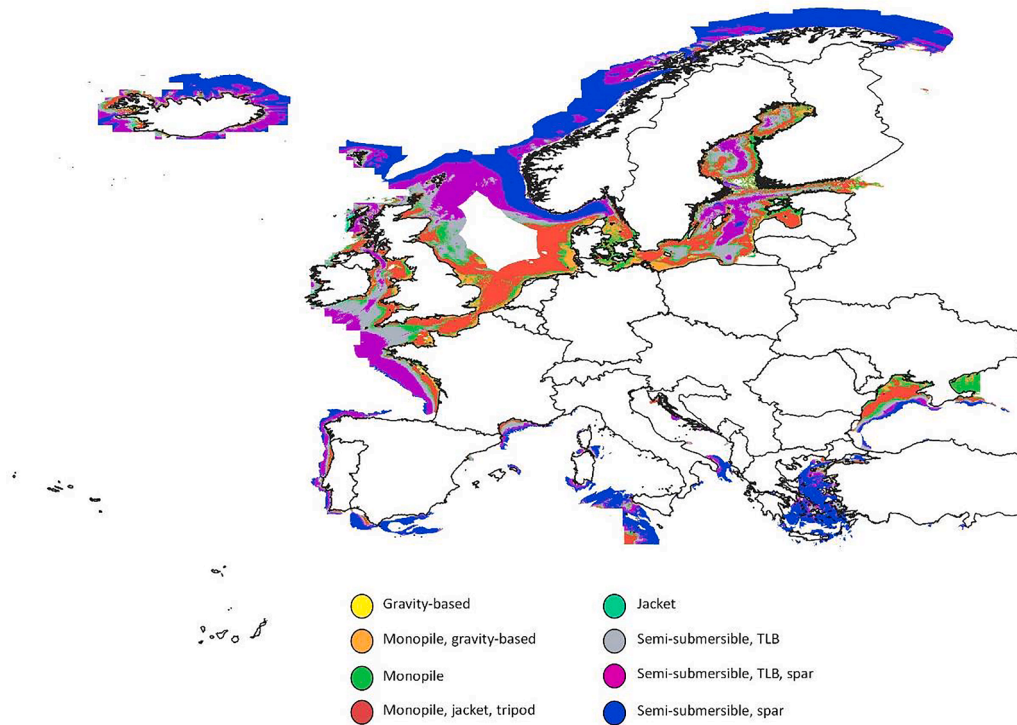


Fig. 10. Map of the most adequate type of foundation in European seas.

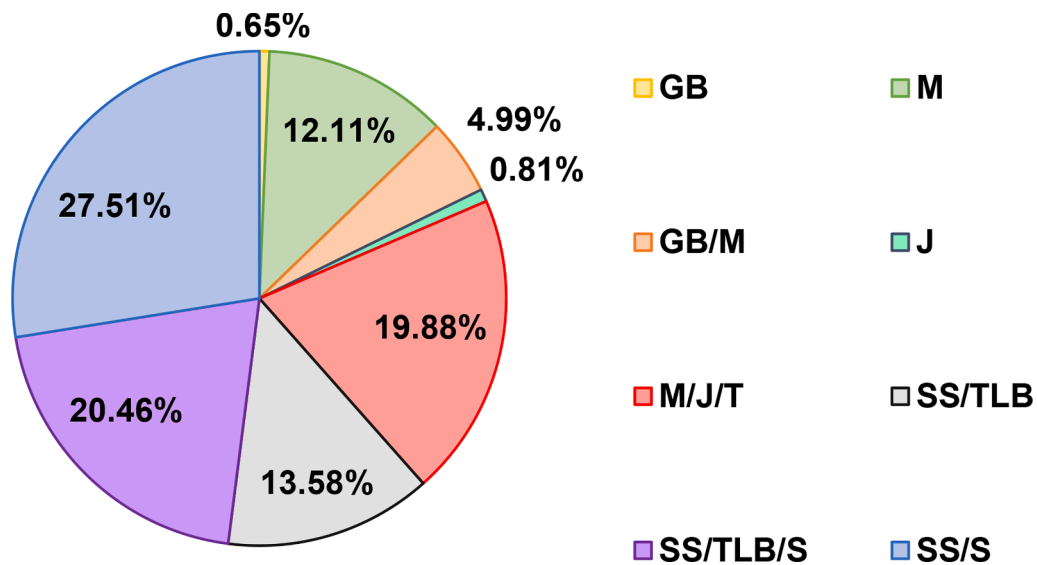


Fig. 11. Potential foundation type distribution for the studied area, where GB: gravity-based, M: monopile, J: jacket, T: tripod, SS: Semi-Submersible, TLB: Tension-Leg-Buoy and S: spar-type support.

*Validation of the results*

The results obtained in the present study have been validated with the type of substructure used in 102 European offshore wind farms. In this way, the location of each of these OWFs has been introduced in the map, to be compared with the theoretical substructure obtained in Fig. 10. This comparison shows a high accuracy in the case of monopiles (94.74 %) and tripods (100 %), although in the case of gravity-based and jackets this accuracy decreases. However, it is worth mentioning that in the case of gravity-based structures, most of the OWFs with this type of structure were commissioned in the early 2000s. As it is well known, the development of monopiles has made this type of structure the most used

one, managing to replace gravity-based structures and, currently, taking their place. For this reason, while gravity-based structures were widely used at the beginning of the century due to the influence of oil & gas structures, today monopiles have gained ground, proving to be a more suitable structure as evidenced in this study. Nonetheless, and all in all, according to the present work, from the 102 analyzed OWFs, the 82.35 % present the most suitable type of foundation. This percentage would increase up-to a value of 89.22 % if the gravity-based structures had been constructed with a monopile type foundation, as it would have probably been done if these were assembled today, and as this study suggests.

It is essential to bear in mind that the results of this study are purely

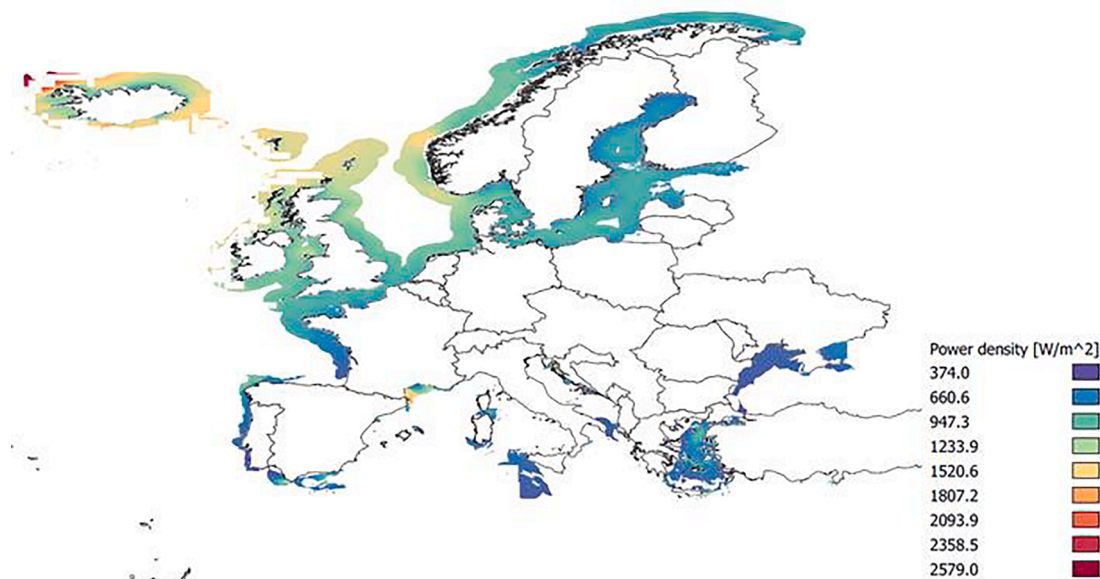


Fig. 12. Mean wind power density (W/m<sup>2</sup>).

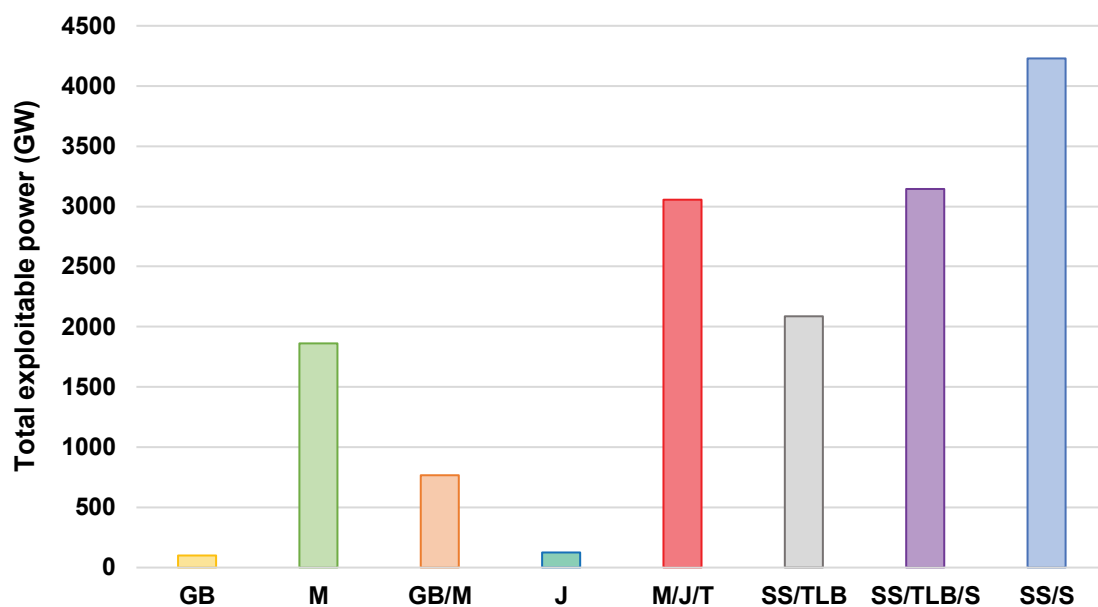


Fig. 13. Total exploitable power for each group of foundations, where GB: gravity-based, M: monopile, J: jacket, T: tripod, SS: Semi-Submersible, TLB: Tension-Leg-Buoy and S: spar-type support.

theoretical and that, to be a true representation of reality, other aspects should be taken into consideration. The aim of this work has been to provide a preliminary overview of the types of structures that are feasible in European seas, considering certain geotechnical and met-ocean parameters.

One of the most important aspects to consider is cost. The cost of the substructure itself represents 22 % of the total CAPEX, so that variations between the different types can lead to significant differences in the total cost of a project. As stated by [56,57] the cost is strongly dependent on the water depth and the seabed characteristics, and to a minor extent, on the turbine capacity and the wave conditions. In most previous studies [9,48,58], the cost of the substructure ( $C_F$ ) is only shown as a function of depth ( $D$ ). From these studies, [57] established a polynomial relationship between the depth and the cost of the substructure in the case of monopiles and jackets, and linear in the case of TLBs (see Eq. (2) and

Table 6).

$$C_F = aD^2 + bD + c \tag{2}$$

Other studies [59] have presented simplified equations in the case of floating structures, although in these cases parameters such as waves have to be considered.

However, beyond the CAPEX there are other costs to be considered, such as the installation and subsequent operation and maintenance of the wind farm, or the visual and environmental impact that the wind farm may have. In [60] a multi-objective optimization based on Pareto fronts is performed, considering both the economic factors and the visual impact of the wind farm itself, thus offering a guide to follow when designing a wind farm.

In addition to this, it is crucial to study the costs of decommissioning the wind farm once it has reached the end of its service life. DECEX costs

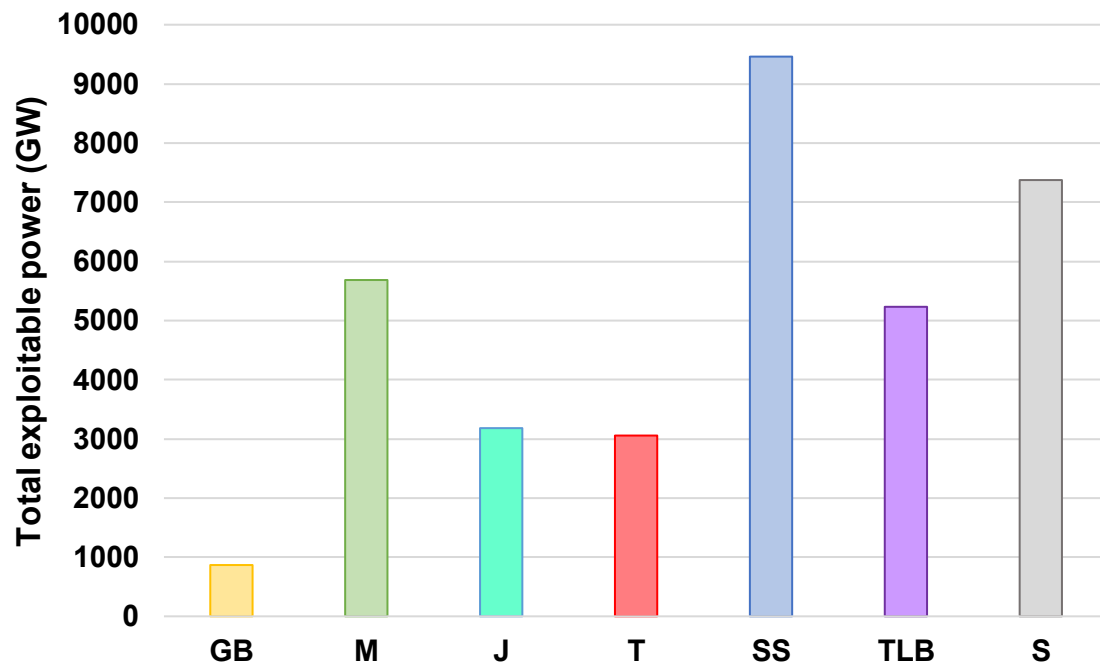


Fig. 14. Total exploitable power for each type of foundation, where GB: gravity-based, M: monopile, J: jacket, T: tripod, SS: Semi-Submersible, TLB: Tension-Leg-Buoy and S: spar-type support.

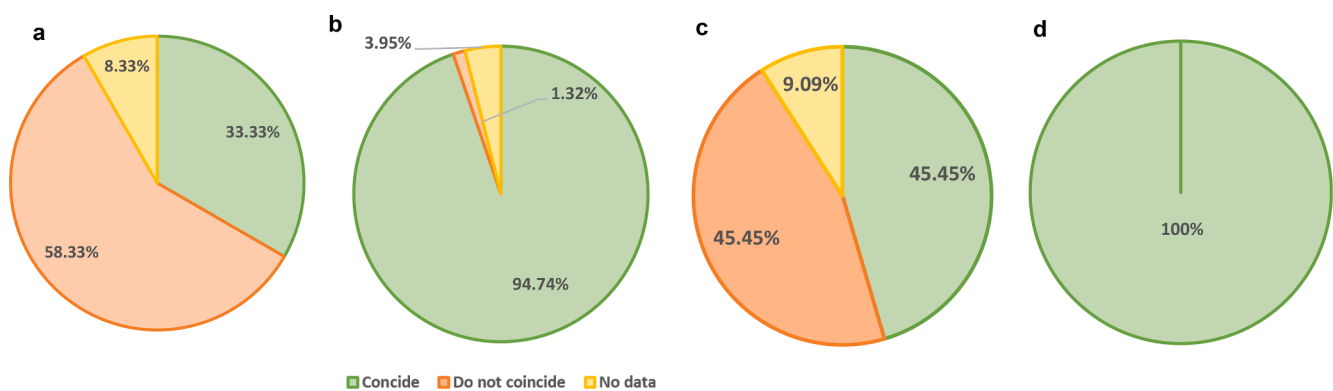


Fig. 15. Foundation adequateness of European Offshore Wind Farms. a) Gravity-based, b) Monopiles, c) Jackets, d) Tripods.

Table 6

Parameters that represent the evolution of foundation costs as a function of water depth [57].

| Foundation type | Depth range [m] | Functional parameters |           |         |
|-----------------|-----------------|-----------------------|-----------|---------|
|                 |                 | a                     | b         | c       |
| Monopile        | 0 – 25          | 201.00                | 612.93    | 411,464 |
| Jacket          | 25 – 55         | 114.24                | -2,270.00 | 531,738 |
| TLB             | 55 – 1000       | 0.00                  | 773.85    | 680,651 |

comprise decommissioning costs of the entire infrastructure previously installed and exploited, and the clearance of the site used for that purpose. These costs may vary between 1.2 % and 8 % of the total costs for an offshore wind farm project, being dependent on whether the structures are bottom-fixed or floating [61–64].

In [65] a new cost approach is presented, by adding decommissioning costs to the existing CAPEX and OPEX. Taking the information from the oil & gas industry as a reference, the proposed model considers both the transport and the total removal of the elements that make up an offshore wind farm. This study allows to have a global vision

of all the factors and costs involved in this type of projects from the beginning, so that the decision making regarding the type of substructure is more precise, thus achieving a cost optimization.

### Conclusions

In this work, the influence of the different geotechnical and met-ocean parameters (water depth, soil substrate, wind speed, and wave energy flux) affecting the determination of the type of offshore wind structures has been analyzed. By means of a GIS, a MCDM model based on the aforementioned parameters has been implemented, allowing to determine the most adequate type of offshore wind foundation. The obtained results have been figured in a complete European map containing all the types of offshore foundations, elucidating which of them is the most appropriate to implement depending on the area. Moreover, the theoretically total exploitable offshore wind power of Europe has been determined, defining the total amount of turbines that could be installed.

Floating offshore wind is called to head the offshore wind installations in Europe, as the area available for these installations is 1,314,004 km<sup>2</sup>, which corresponds to the 61.55 % of the total



considered available area. On the other hand, among the fixed structures, the monopile is positioned as the main option to use in European seas, as it can be sited in the 36.98 % of the area analyzed. In the case of floating structures, semi-submersibles (61.55 %) and spar-type supports (47.97 %) take the lead over TLBs. The theoretically total exploitable power by offshore wind in Europe is 15.37 TW, which could be achieved by installing 1,024,667 of V236-15.0 MW type turbines with a nominal power of 15 MW. This would increase to 615 times the current offshore wind installed power in Europe [66]. The most suitable areas for implementing offshore projects, given the limitations established by wind speed, are located in the North Sea (on the Dutch coast and on the west coast of Denmark and Norway), on the east coast of Great Britain, on the Atlantic coast of Galicia and in the north Mediterranean Sea area between Girona and Marseille.

Future studies will continue analyzing the direct influence of CAPEX on the decision of the substructure selection. In addition, the obtained results will be compared with real experimental data for a further validation.

### CRedit authorship contribution statement

**Asier Vázquez:** Conceptualization, determination of criteria and bibliographic review, development of the GIS methodology, and original draft preparation. **Urko Izquierdo:** Conceptualization, Writing – review & editing, Supervision. **Peter Enevoldsen:** Conceptualization, Validation, Writing – review & editing, Supervision. **Finn-Hendrik Andersen:** Methodology, Writing – review & editing. **Jesús María Blanco:** Conceptualization, Supervision, Methodology.

### Declaration of Competing Interest

The authors declare that they have no known competing financial interests or personal relationships that could have appeared to influence the work reported in this paper.

### Data availability

The authors do not have permission to share data.

### Acknowledgements

Authors would like to thank the University of the Basque Country (UPV/EHU) and the Basque Government through the research group (IT1514-22).

### References

- [1] Wind Europe, History of Europe's wind industry, (2021). <https://windeurope.org/about-wind/history/timeline/one-of-the-first-wind-turbines/> (accessed August 31, 2021).
- [2] IRENA, Wind Energy Data, (2022). <https://www.irena.org/wind> (accessed July 18, 2022).
- [3] Enevoldsen P, Xydis G. Examining the trends of 35 years growth of key wind turbine components. *Energy Sustain. Dev.* 2019;50:18–26.
- [4] Enevoldsen P, Permien FH, Bakhtaoui I, von Krauland AK, Jacobson MZ, Xydis G, et al. How much wind power potential does Europe have? Examining European wind power potential with an enhanced socio-technical atlas. *Energy Policy* 2019; 132:1092–1100. <https://doi.org/10.1016/j.enpol.2019.06.064>.
- [5] Heptonstall P, Gross R, Greenacre P, Cockerill T. The cost of offshore wind: Understanding the past and projecting the future. *Energy Policy* 2012;41:815–21.
- [6] Arany L, Bhattacharya S, Macdonald J, Hogan SJ. Design of monopiles for offshore wind turbines in 10 steps. *Soil Dyn. Earthq. Eng.* 2017;92:126–52.
- [7] Sovacool BK, Enevoldsen P, Koch C, Barthelmie RJ. Cost performance and risk in the construction of offshore and onshore wind farms. *Wind Energy* 2017;20(5): 891–908.
- [8] The Wind Power, The Wind Power, (2019). <https://www.thewindpower.net/index.php> (accessed August 31, 2021).
- [9] Myhr A, Bjerkseter C, Ågotnes A, Nygaard TA. Levelized cost of energy for offshore floating wind turbines in a lifecycle perspective. *Renew. Energy* 2014;66:714–28. <https://doi.org/10.1016/j.renene.2014.01.017>.
- [10] Wind Europe, Unleashing Europe's offshore wind potential, 2017.
- [11] Wind Europe, Wind energy in Europe. 2021 Statistics and the outlook for 2022–2026, 2022.
- [12] W. Musial, D. Heimiller, P. Beiter, G. Scott, C. Draxl, 2016 Offshore Wind Energy Resource Assessment for the United States, (2016) 88.
- [13] Enevoldsen P, Jacobson MZ. Data investigation of installed and output power densities of onshore and offshore wind turbines worldwide. *Energy. Sustain Dev* 2021;60:40–51. <https://doi.org/10.1016/j.esd.2020.11.004>.
- [14] Wind Power Offshore, Stiesdal's Tetra Spar set for demonstration, (2018). <https://www.windpoweroffshore.com/article/1495141/stiesdals-tetraspar-set-demonstration> (accessed August 31, 2021).
- [15] Bento N, Fontes M. Emergence of floating offshore wind energy: Technology and industry. *Renew. Sustain. Energy Rev.* 2019;99:66–82.
- [16] Kim T, Park J-I, Maeng M. Offshore wind farm site selection study around Jeju Island, South Korea. *Renew Energy* 2016;94:619–28.
- [17] Kausche M, Adam F, Dahlhaus F, Großmann J. Floating offshore wind – Economic and ecological challenges of a TLP solution. *Renew. Energy* 2018;126:270–80. <https://doi.org/10.1016/j.renene.2018.03.058>.
- [18] M. Tolon, D.N. Ural, Geotechnical Considerations for Offshore Wind Turbines based on Neural Network, in: Adv. Civ. Environ. Mater. Res., 2012: pp. 3265–3276.
- [19] Wang X, Zeng X, Li J, Yang X, Wang H. A Review on Recent Advancements of Substructures for Offshore Wind Turbines. *Energy Convers Manag* 2018.
- [20] Chakrabarti SK. *Ocean Environment* 2005:79–131.
- [21] EMODnet, EMODnet, (2021). <https://emodnet.eu/en> (accessed January 13, 2021).
- [22] Long D. Seabed sediment classification 2006.
- [23] Global Wind Atlas, GLOBAL WIND ATLAS, Glob. Sol. Atlas | Energydata.Info. (2021). <https://globalwindatlas.info/> (accessed April 18, 2021).
- [24] Copernicus, ECMWF, Climate Change Service, ERA5 hourly data on single levels from 1979 to present, 2021. <https://cds.climate.copernicus.eu/cdsapp#!/dataset/reanalysis-era5-single-levels?tab=form> (accessed May 20, 2021).
- [25] Europe W. Offshore wind in Europe statistics 2021 2020.
- [26] Sparrevik P. Offshore Wind Turbine Foundations State of the Art. Res. to Appl. Geotech. 2019.
- [27] L. Hammar, S. Andersson, R. Rosenberg, Adapting offshore wind power foundations to local environment, 2010.
- [28] ETIP, Floating Offshore Wind. Delivering Climate Neutrality, 2020.
- [29] International Renewable Energy Agency (IRENA), Floating Foundations: A Game Changer for Offshore Wind Power, (2016) 1–8. [http://www.irena.org/-/media/Files/IRENA/Agency/Publication/2016/IRENA\\_Offshore\\_Wind\\_Floating\\_Foundations\\_2016.pdf](http://www.irena.org/-/media/Files/IRENA/Agency/Publication/2016/IRENA_Offshore_Wind_Floating_Foundations_2016.pdf).
- [30] S. Bradley, Offshore Wind Floating Wind Technology Key headlines, Energy Technol. Inst. (2015).
- [31] P.L.C. Van der Valk, Coupled Simulations of Wind Turbines and Offshore Support Structures: Strategies based on the Dynamic Substructuring Paradigm, 2019. [https://www.researchgate.net/publication/275213625\\_Coupled\\_Simulations\\_of\\_Wind\\_Turbines\\_and\\_Offshore\\_Support\\_Structures\\_Strategies\\_based\\_on\\_the\\_Dynamic\\_Substructuring\\_Paradigm](https://www.researchgate.net/publication/275213625_Coupled_Simulations_of_Wind_Turbines_and_Offshore_Support_Structures_Strategies_based_on_the_Dynamic_Substructuring_Paradigm).
- [32] Moore A, Price J, Zeyringer M. The role of floating offshore wind in a renewable focused electricity system for Great Britain in 2050. *Energy Strateg. Rev.* 2018;22: 270–8. <https://doi.org/10.1016/j.esr.2018.10.002>.
- [33] Arent D, Sullivan P, Heimiller D, Lopez A, Eurek K, Badger J, et al. Improved Offshore Wind Resource Assessment in Global Climate Stabilization Scenarios. *Natl. Renew. Energy Lab.* 2012;29. <https://www.nrel.gov/docs/fy13osti/55049.pdf>.
- [34] M. Keene, Comparing offshore wind turbine foundations, (2021). <https://www.windpowerengineering.com/comparing-offshore-wind-turbine-foundations/> (accessed March 10, 2021).
- [35] BOEM. Comparison of Environmental Effects from Different Offshore Wind Turbine Foundations. Paper-Final-White-Paper.pdf; 2020. p. 1–42.
- [36] R. James, M. Costa Ros, Floating Offshore Wind: Market and Technology Review, 2015. [https://prod-dupal-files.storage.googleapis.com/documents/resource/public/Floating Offshore Wind Market Technology Review – REPORT.pdf](https://prod-dupal-files.storage.googleapis.com/documents/resource/public/Floating%20Offshore%20Wind%20Market%20Technology%20Review%20-%20REPORT.pdf).
- [37] S. Butterfield, W. Musial, J. Jonkman, P. Sclavounos, L. Wayman, Engineering Challenges for Floating Offshore Wind Turbines By, Process. Fee to U.S. Dep. Energy Its Contract. (2007). <http://www.osti.gov/bridge%5CnAvailable>.
- [38] Taboada J. Comparative analysis review on Floating Offshore wind Foundations (FOFW). *Ing. Nav.* 2016;75–87.
- [39] DNV. Guideline for Offshore Structural Reliability Analysis – Application to Tension Leg Platforms. 1995.
- [40] DNV, The Crown Estate – UK Market Potential and Technology Assessment for floating offshore wind power. An assessment of the commercialization potential of the floating offshore wind industry. DNV. (2012). <https://pelastar.com/wp-content/uploads/2015/04/uk-floating-offshore-wind-power-report.pdf>.
- [41] Leimeister M, Kolios A, Collu M. Critical review of floating support structures for offshore wind farm deployment. *J. Phys. Conf. Ser.* 2018;1104. <https://doi.org/10.1088/1742-6596/1104/1/012007>.
- [42] von Krauland A-K, Permien F-H, Enevoldsen P, Jacobson MZ. Onshore wind energy atlas for the United States accounting for land use restrictions and wind speed thresholds. *Smart Energy* 2021;3:100046. <https://doi.org/10.1016/j.segy.2021.100046>.
- [43] Global Wind Atlas, Key Features, Glob. Sol. Atlas | Energydata.Info. <https://globalwindatlas.info/about/method> (accessed April 20, 2021).
- [44] E. Paya, A. Zigeng Du, The frontier between fixed and floating foundations in offshore wind, *Emp. Eng.* (2020). <https://www.empireengineering.co.uk/the-frontier-between-fixed-and-floating-foundations-in-offshore-wind/> (accessed April 22, 2021).



- [45] Herbich JB. Wave energy and wave energy flux, in: *Handb. Coastal Eng.* McGraw Hill; 2000.
- [46] Yang J, He YP, Zhao YS, Shao YL, Han ZL. Experimental and numerical studies on the low-frequency responses of a spar-type floating offshore wind turbine. *Ocean Eng.* 2021;222:108571. <https://doi.org/10.1016/j.oceaneng.2021.108571>.
- [47] Chuang T-C, Yang W-H, Yang R-Y. Experimental and numerical study of a barge-type FOWT platform under wind and wave load. *Ocean Eng.* 2021;230:109015. <https://doi.org/10.1016/j.oceaneng.2021.109015>.
- [48] Collu M, Borg M. Design of floating offshore wind turbines. Elsevier Ltd 2016. <https://doi.org/10.1016/B978-0-08-100779-2.00011-8>.
- [49] Ampah JD, Yusuf AA, Afrane S, Jin C, Liu H. Reviewing two decades of cleaner alternative marine fuels: Towards IMO's decarbonization of the maritime transport sector. *J. Clean. Prod.* 2021;320:128871. <https://doi.org/10.1016/j.jclepro.2021.128871>.
- [50] Yusuf AA, Dankwa Ampah J, Soudagar MEM, Veza I, Kingsley U, Afrane S, et al. Effects of hybrid nanoparticle additives in n-butanol/waste plastic oil/diesel blends on combustion, particulate and gaseous emissions from diesel engine evaluated with entropy-weighted PROMETHEE II and TOPSIS: Environmental and health risks of plastic wa. *Energy Convers. Manag.* 2022;264:115758. <https://doi.org/10.1016/j.enconman.2022.115758>.
- [51] QGIS. QGIS.com (accessed November 14, 2021).
- [52] GWEC, Global Offshore Wind Report 2021, 2022. <https://gwec.net/wp-content/uploads/2021/03/GWEC-Global-Wind-Report-2021.pdf>.
- [53] Martinez A, Iglesias G. Multi-parameter analysis and mapping of the levelised cost of energy from floating offshore wind in the Mediterranean Sea. *Energy Convers. Manag.* 2021;243:114416. <https://doi.org/10.1016/j.enconman.2021.114416>.
- [54] Martinez A, Iglesias G. Site selection of floating offshore wind through the levelised cost of energy: A case study in Ireland. *Energy Convers. Manag.* 2022;266:115802. <https://doi.org/10.1016/j.enconman.2022.115802>.
- [55] Martinez A, Iglesias G. Mapping of the levelised cost of energy for floating offshore wind in the European Atlantic. *Renew. Sustain. Energy Rev.* 2022;154:111889. <https://doi.org/10.1016/j.rser.2021.111889>.
- [56] Gonzalez-Rodriguez AG. Review of offshore wind farm cost components. *Energy Sustain. Dev.* 2017;37:10–9. <https://doi.org/10.1016/j.esd.2016.12.001>.
- [57] Bosch J, Staffell I, Hawkes AD. Global levelised cost of electricity from offshore wind. *Energy* 2019;189:116357. <https://doi.org/10.1016/j.energy.2019.116357>.
- [58] M. Seidel, Substructures for offshore wind turbines – Current trends and developments, *Festschrift Peter Schaumann.* (2014) 363–368. <https://doi.org/10.2314/GBV>.
- [59] Cavazzi AGDS. An Offshore Wind Energy Geographic Information System (OWE-GIS) for assessment of the UK's offshore wind energy potential. *Renew. Energy* 2016;87:212–28.
- [60] Gonzalez-Rodriguez AG, Serrano-Gonzalez J, Burgos-Payan M, Riquelme-Santos J. Multi-objective optimization of a uniformly distributed offshore wind farm considering both economic factors and visual impact. *Sustain. Energy Technol. Assessments* 2022;52:102148. <https://doi.org/10.1016/j.seta.2022.102148>.
- [61] Maienza C, Avossa AM, Ricciardelli F, Coiro D, Troise G, Georgakis CT. A life cycle cost model for floating offshore wind farms. *Appl. Energy* 2020;266:114716. <https://doi.org/10.1016/j.apenergy.2020.114716>.
- [62] BVG associates, Offshore Wind anticipated innovations impact 2017, (2017).
- [63] Climate Change Capital, Offshore Renewable Energy Installation Decommissioning Study, (2017).
- [64] Topham E, McMillan D. Sustainable decommissioning of an offshore wind farm. *Renew. Energy* 2017;102:470–80. <https://doi.org/10.1016/j.renene.2016.10.066>.
- [65] Milne C, Jalili S, Maheri A. Decommissioning cost modelling for offshore wind farms: A bottom-up approach. *Sustain. Energy Technol. Assessments* 2021;48:101628. <https://doi.org/10.1016/j.seta.2021.101628>.
- [66] REN21, Renewables 2020 Global status report, 2021.